



## CANCER DETECTION USING METAMATERIAL BIOSENSOR IN THE TERAHERTZ REGIME

A. Zaheetha Banu<sup>1</sup>, Zara Chemseddine<sup>2</sup>, K. S. Joseph Wilson<sup>3</sup>

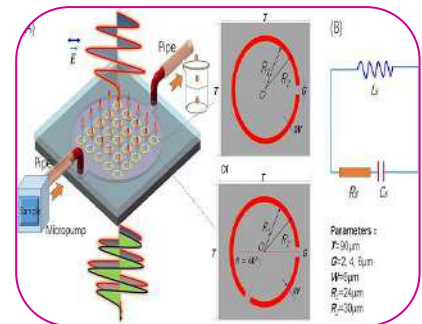
<sup>1</sup>Department of Physics, Manonmaniam Sundaranar University, Abishekapatti, Tirunelveli, Tamilnadu, India.

<sup>2</sup>University of Brothers' Mentouri Constantine 1, Algeria.

<sup>3</sup>Department of Physics, Arul Anandar College, Karumathur, Madurai.

### ABSTRACT

A split ring resonator based metamaterial structure is designed, simulated, and investigated as a biosensor in this article for efficient detection of breast cancer. In our proposed resonator structure we can see a remarkable high shifting in resonance frequencies peaks shows us to detect the normal and various cancer cells and also shows us the low shifting between cells. We have obtained the resonance frequency value as 0.601THz with an attenuation of -30dB from the simulated results which allow us to detect cancer cell in terahertz range and obtained the sensitivity of the biosensor of the biological molecules equal to 0.058 THz (58 GHz) and along with this the specific absorption rate is obtained in the THz region by means of extensive finite element method (FEM) using COMSOL Multiphysics 5.3. By using mathematical interpolation based of fitting methods of the 4<sup>th</sup> and 5<sup>th</sup> order the variation of thickness of various breast cancer cells as function of resonance frequencies peaks were plotted by using Matlab software. In this paper, we have also introduced Nicolson Ross-Weir method (NRW) method to achieve negative electrical permittivity and negative magnetic permeability in a split ring resonator based metamaterial in the THz region. Our simulation outcomes indicate a remarkable high sensor functionality of the SRR biosensor devices. Finally, we showed that the metamaterial based split ring resonator sensor possesses much higher sensitivity to detect cancer cells for cancer diagnosis.



**KEYWORDS :** metamaterials, split ring resonator, biosensor, finite element method simulation, Nicolson Ross-Weir method (NRW)

### 1. INTRODUCTION

Metamaterials were first introduced by Veselago in 1968[1].metamaterials is known as artificially engineered materials. Artificially engineered metamaterials have emerged with interesting properties and functionalities previously unattainable in natural materials. An obscure behaviour of these novel metamaterials is interesting field of research and researchers who are devoted to finding characteristics of metamaterial from both fundamental and Practical point of view. During recent years, metamaterials have generated a tremendous amount of research interest due to their extraordinary response to electromagnetic waves. Metamaterials are engineered materials that typically have periodically arranged features of dimensions smaller than that of the wavelength of light. They demonstrate electromagnetic properties quite different from those of naturally occurring materials.

Electromagnetic waves in the terahertz (THz) frequency range have received tremendous attention Owing to the relation between metamaterial science and sensing technology. Apart from interesting physics and novel electromagnetic phenomena the metamaterials offers great opportunities to realize several ground-breaking engineering applications such as Sub diffraction Imaging[2], invisibility cloaks[3], chemical

and bimolecular sensing[4,5], have generated over a relatively enormous interest in metamaterials. Recently, great interest has been ardent to sensing applications of metamaterials. Jakšić et al. [6] metamaterials convenient for Plasmon-based chemical sensing with enhanced sensitivity investigated with some peculiarities of electromagnetic, and they envisioned the practical applications of metamaterial-based sensors in bio sensing, chemical sensing, environmental sensing, homeland security, etc. He et al. [7]. Furthermore, prevalent advances have been realized on the metamaterial based sensors which lead to detecting information of a substance and a situation. Metamaterials that operate in the THz range have attracted fanatical interest of highly desirable THz applications in high-sensitivity sensing.

Split-ring resonators (SRR) are possibly the most common metamaterial structural unit and are utilised for their resonant response and negative magnetic properties. The Split Ring Resonator (SRR) is one such nanostructure that forms the basic unit of a metamaterial [8]. Sensors have to meet some requirements in order to work effectively. For example, they must have a loss factor as low as possible to prevent substrate absorption. The sensors must give a measurable signal according to the changes in the parameters. The sensor must shift the resonance frequency sharply according to the quantity of the changes in the observed parameter. Related shifts can easily be observed if the sensor sensitivity is high. The permittivity of the dielectric substrate has gained an essential role and needs accurate evaluation in different range of frequencies. The proposed desired resonator has a sample structure, easy to enhance the sensor's performance with respect to the material characterization. These suggested requirements are considered and realized in this study to obtain a new sensor based on a metamaterial designed by desired split ring resonator.

The purpose of this paper is to investigate the performance of metamaterial based split ring resonator as sensor used for detecting the cancer cells for cancer diagnosis. Cancer is the second largest disease throughout the world even if it is not identified at the earlier stage it will leads to the increasing mortality rate. Statistics reveal that around 13.2 million deaths of cancer are expected in 2030 [9]. Early detection of cancer is an important aspect for effective treatment. Detection of cancer can be done in various ways and usually depends on the stage in which the cancer cell growth is traced.

The patient's survival rate is uncertain due to the limitations of cancer diagnosis and therapy. Early diagnosis of cancer is crucial for its successful treatment. A biomarker-based cancer diagnosis may extensively improve the early diagnosis and subsequent treatment. Biosensors play a crucial role in the detection of biomarkers as they are easy to use, portable, and can do analysis in real time. Our proposed desired structure of metamaterial based split ring resonator sensor designed. The sensors highlight analytical and simulated performances of various cancer cells in detail. . In this research, we explore dynamically the novel concepts of metamaterials based split ring resonator with high sensitivity have been realized for sensing to address the shift in frequency range [THz] is of special interest to detect malignancy in biological cells and tissues for cancer diagnosis. Accurate diagnosis and treatment have always been a challenging task. The finite element method (FEM) using COMSOL Multiphysics version 5.3 is used to analyze the various properties of biosensors and the characterization of the biosensor based on scattering parameters (S-parameters) of transmission and reflection coefficients. Sensors built using metamaterials based split ring resonator shows high sensitivity. Finally, we showed that the metamaterial based split ring resonator sensor possesses much higher sensitivity to detect cancer cells for cancer diagnosis.

Hence metamaterials offers more exciting and challenging possibilities for novel electromagnetic responses and this research is to be encouraged to continue to utilize their properties for various applications ranging from optical biosensing and this is expected to achieve exponential growth over the upcoming years.

## 2. SENSOR DESIGN AND WORKING PRINCIPLE:

In this paper we have designed and studies a biosensor device based on metamaterial SRR structure for operation in the terahertz regime (THz). The proposed structure of metamaterial based split ring

resonator as biosensor possesses much higher sensitivity to detect the cancer cells for cancer diagnosis. The figure (Fig.1) Shows the layout of the thin copper layer design of metamaterial resonator structure and the Unit cell of biosensor based of metamaterials is shown in the figure (Fig .2), this complex structure is designed by using Comsol Multiphysics 5.3.

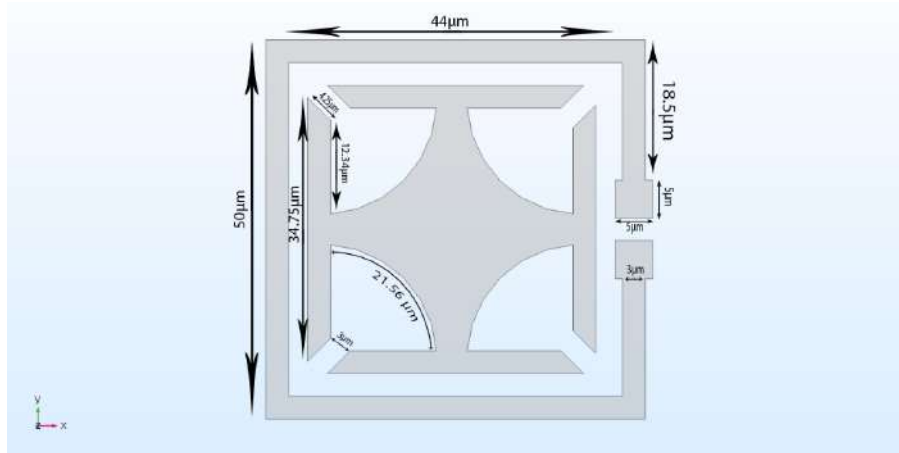


**FIG.1. THE THIN COPPER LAYERS DESIGN OF**

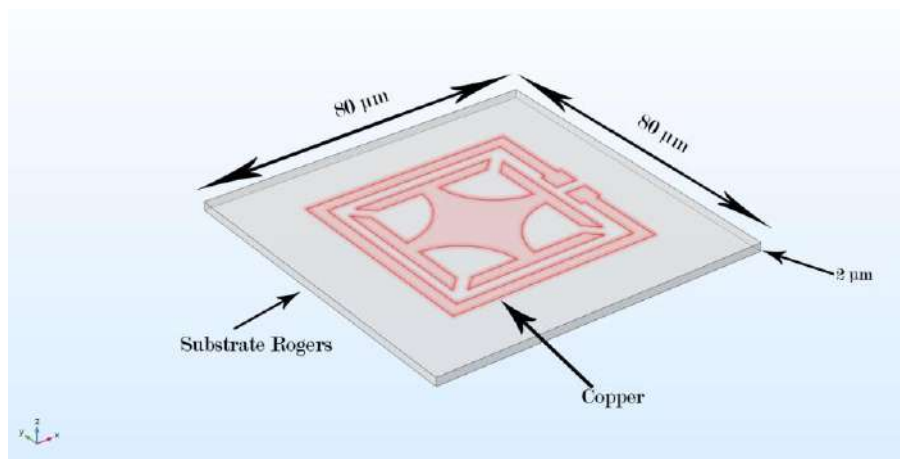


**FIG.2. UNIT CELL OF BIOSENSOR BASED ON METAMATERIALS**

The proposed metamaterial structure is designed by the substrate material composed of Rogers (RO4003C) with dielectric constant ( $\epsilon_r=2.8$ ) and electrical conductivity  $\sigma = 5.88 * 10^{-11} S/m$  . The thickness of substrate is 2  $\mu m$ , and its length and width are equal to 80 $\mu m$  is shown in the figure (Fig.2). The SRR is made up of a very thin layer of copper material with dielectric constant ( $\epsilon_r=1$ ) and electrical conductivity $\sigma = 5.96 * 10^7 S/m$ . . The proposed resonator structure is placed in a waveguide of vacuum by having its length and widths are equal to 80 $\mu m$  along with the height of 400 $\mu m$ . The Placement of the Resonator in a waveguide is shown in the figure (Fig.3).

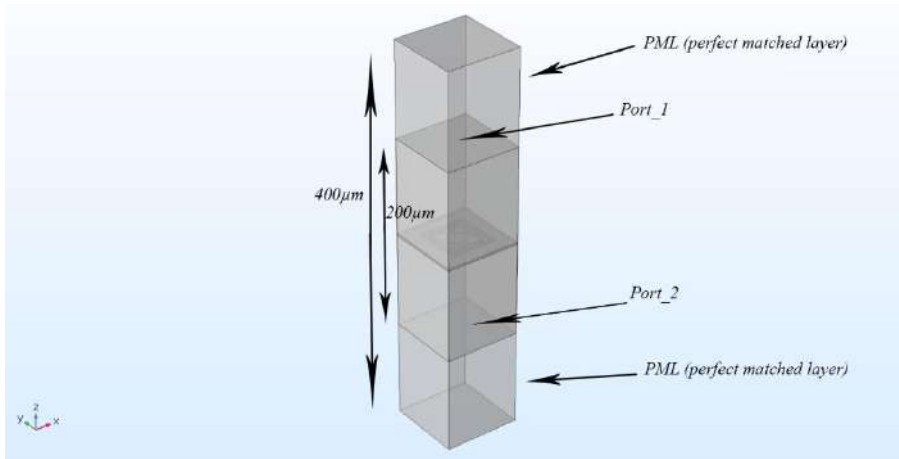


**Fig.3. Placement of the Resonator in a waveguide**

The working principle of the biosensor device based on metamaterial SRR structure can be easily demonstrated by analyzing the scattering parameters of the device [10]. The transmission parameter  $S_{21}$  and the reflectance parameters  $S_{11}$  both are strongly depend on the frequency. The biosensors highlight analytical and simulated performances to detect the normal and various cancer cells in detail with remarkable high shifting in resonance frequencies and the low shifting between cells.

**3. SIMULATION CONFIGURATION**

In this section, we present here the following steps to characterize the metamaterials by the simulation of COMSOL Multiphysics environment version 5.3. The method used in this simulation is Finite Element Method (FEM) and this method uses the s-parameters of the metamaterial to extract the characteristics. The finite element method (FEM) is used to analyze the various properties of biosensors [11]. In this simulation study, we use the Finite Element Method to solve the following equations in the frequency domain:

$$\nabla \times \mu_r^{-1}(\nabla \times E) - k_0^2 \left( \epsilon_r - \frac{j\sigma}{\omega\epsilon_0} \right) E = 0 \quad (1)$$

$$E(x, y, z) = \tilde{E}(x, y)e^{-jk_z z} \quad (2)$$

Where  $\mu_r$  and  $\epsilon_r$  are the relative permeability and permittivity,  $\sigma$  the electric conductivity tensor,  $\omega$  the angular frequency,  $k_0$  the wave number in free space and  $\epsilon_0$  is vacuum dielectric constant.

The characterization of the biosensor based of its transmission and reflection parameters given by the scattering parameters (S-parameters) that given by the following equations:

$$S_{11} = \frac{\int_{port\ 1} ((E_c - E_1) \cdot E_1^*) \cdot dA_1}{\int_{port\ 1} (E_1 \cdot E_1^*) \cdot dA_1} \quad (3)$$

$$S_{21} = \frac{\int_{port\ 2} ((E_c - E_2) \cdot E_2^*) \cdot dA_2}{\int_{port\ 2} (E_2 \cdot E_2^*) \cdot dA_2} \quad (4)$$

Where:  $S_{11}$  : The reflection coefficient at the input port 1.  $S_{21}$  : The transmission coefficient at the output port 2. where,  $E_c$  is the computed electric field on the port consists of the excitation along with the

reflected field,  $E_1$  the electric fields on ports 1,  $E_2$  the electric fields on ports 2.  $dA_1$  and  $dA_2$  are the cross section of the port 1 and port 2.

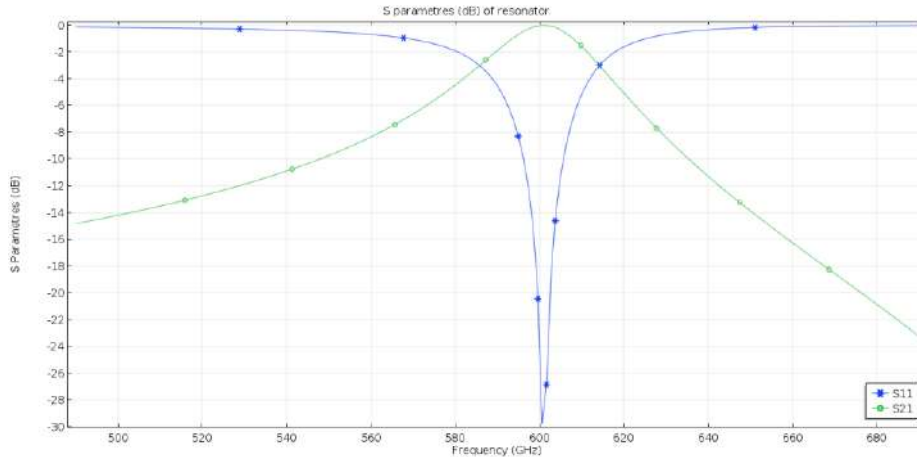


**FIG.4. PARAMETERS S FOR TRANSMISSION  $S_{21}$  AND REFLECTION  $S_{11}$  FOR THE SENSOR WITHOUT SAMPLES.**

As shown in the figure (Fig.4). The resonance frequency of reflection parameter  $S_{11}$  from the curve equal to 0.601 THz with attenuation value of -30dB. In this paper we only interested in the reflection parameter  $S_{11}$  that shown in blue line. The values obtained for the resonance frequency allow us to use this resonator as breast cancer cell detector in terahertz frequency range.

To characterize the metamaterial we have used the method of Nicolson-Ross-Weir (NRW), the effective metamaterial characteristics are extracted by the Nicolson-Ross-Weir (NRW) method. The NRW method is a simple and familiar method to characterize the unknown materials, which we used for characterizing metamaterials. The method uses the scattering parameters  $S_{11}$  and  $S_{21}$  of the metamaterial to extract its characteristics.

The NRW method is mathematically represented by following equations [12]. :

$$\epsilon_r = \frac{2 (1 - (S_{11} + S_{21}))}{jk_0 t (1 + (S_{11} + S_{21}))} \tag{5}$$

$$\mu_r = \frac{2 (1 - (S_{11} - S_{21}))}{jk_0 t (1 + (S_{11} - S_{21}))} \tag{6}$$

$$n = -\sqrt{\epsilon_r \mu_r} \tag{7}$$

Where:  $\epsilon_r$ , The effective permittivity,  $\mu_r$ , The effective permeability,  $t = 2 \mu m$ : The substrate thickness, and  $n$ : refractive index,  $k_0$ : wave number.

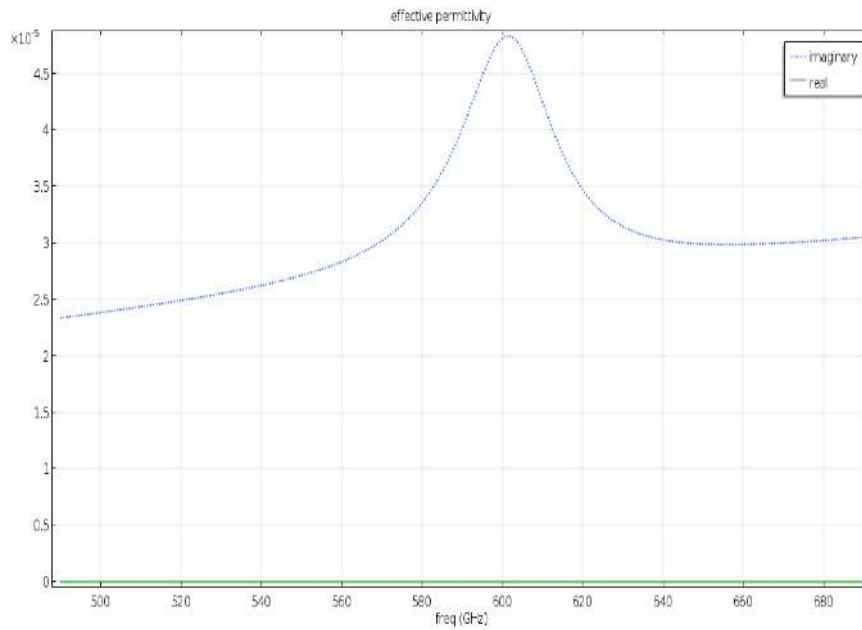


FIG.5.EFFECTIVE PERMITTIVITY GRAPH AS FUNCTION OF FREQUENCY.

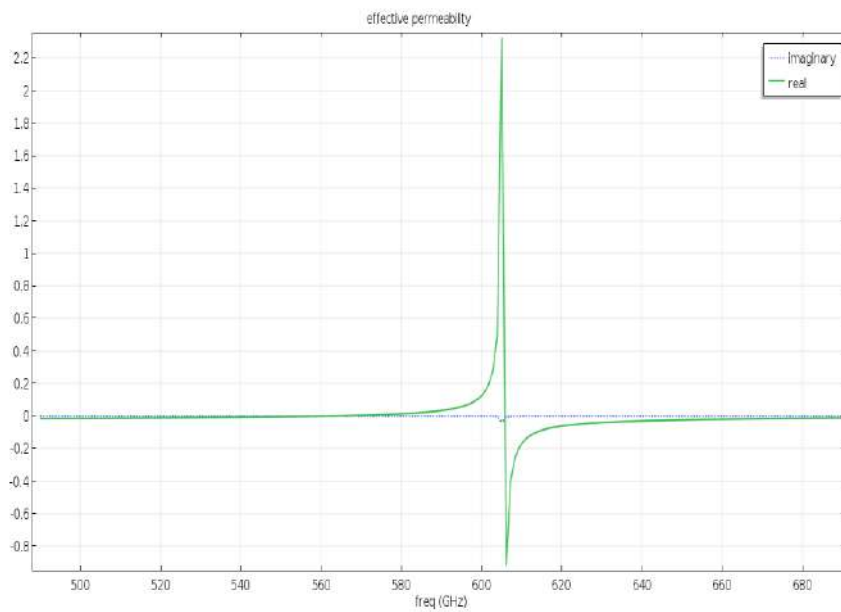
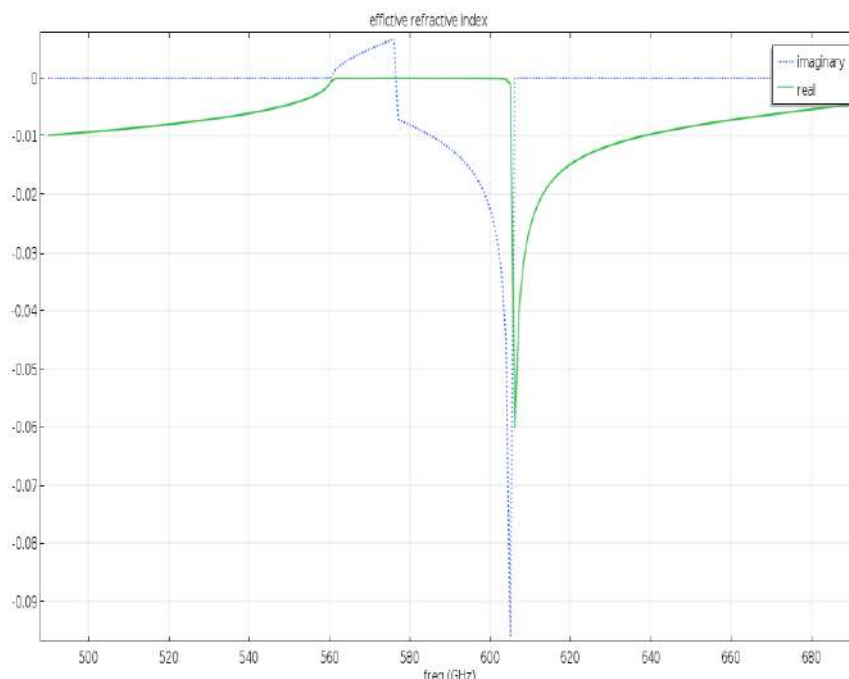


FIG. 6. EFFECTIVE PERMEABILITY GRAPH AS FUNCTION OF FREQUENCY.



**FIG.7.EFFECTIVE REFRACTIVE INDEX GRAPH AS FUNCTION OF FREQUENCY.**

According to the graphs shown in previously cited figures we ensure that we are working with a metamaterial resonator. The electrical permittivity  $\epsilon$  and the magnetic permeability  $\mu$  are the fundamental characteristic quantities that determine the electromagnetic waves propagation in matter. By using the above mathematical equations the metamaterial characteristics of SRR are verified by the figures (Fig. 5, Fig .6) indicates the permittivity ( $\epsilon_r$ ) and the permeability characteristics ( $\mu_r$ ) of SRR of the metamaterial. This structure exhibits both real and imaginary of negative permittivity ( $\epsilon_r$ ), negative permeability ( $\mu_r$ ) which indicates double negative characteristics of SRR metamaterial structure.

As shown in the figures (Fig.5, Fig.6) we that represent a negative permittivity value near to the peak of resonance frequency  $S_{11}$ . That result confirms the negative refractive index as shown in the figure (Fig.7). In the flowing steps we use this table shown below (Table.I) that represent the dielectric constant of normal and cancer cells respectively [13]:

Cells	Dielectric constant
Normal	1.822500
Hela	1.937660
PC-12	1.946025
MDA-MB-231	1.957201
MCF-7	1.962801
Jurkat	1.932100
DLD1	2.018000
Colo-205	2.127300

**TABLE.I.DIELECTRIC CONSTANTS FOR NORMAL AND CANCER CELLS.**

For the last two values (*Table.1*) of colon cancer cells (DLD1, Colo205) is calculated by using Cole-Cole equation with a MATLAB script, we are interested only by the real part of dielectric permittivity given by following equation [14, 15]:

Where:  $\omega = 2\pi f_r$  is the angular frequency and  $f_r$  is the resonance frequency of resonator.

$$\epsilon_r(\omega) = \epsilon_\infty + \frac{\Delta\epsilon(1 + (\omega\tau)^{1-\alpha} \sin^2(\alpha\pi/2))}{1 + 2(\omega\tau)^{1-\alpha} \sin^2(\alpha\pi/2) + (\omega\tau)^{2-\alpha}} \tag{8}$$

$\tau$  : Relaxation time.

$\Delta\epsilon$  : Relaxation strengths.

$\epsilon_\infty = 2$  : Human cell dielectric constant [16, 17].

**4. Simulation results of cancer cell detector:**

In this section, we represent the results given by the simulation of the cancer cell detector based metamaterials, the scattering parameters  $S_{11}$ ,  $S_{21}$  given by the detector with and without normal cell shown in the figure (*Fig.8*).

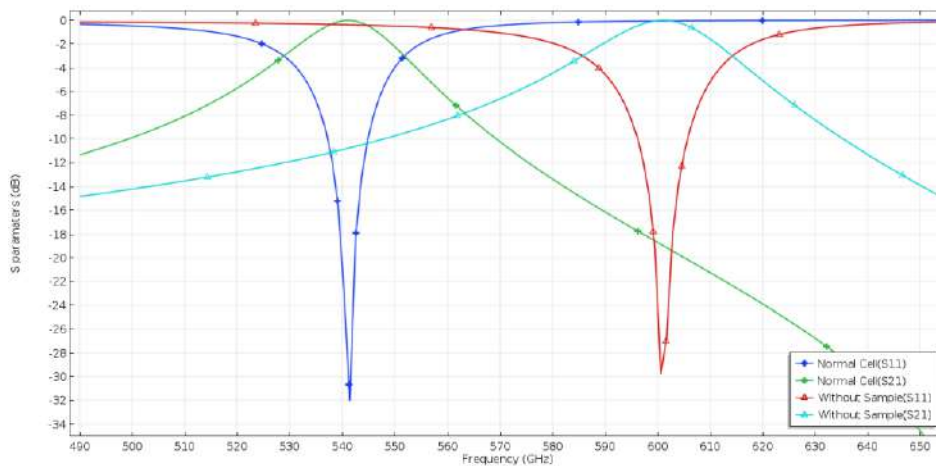


**FIG.8. SCATTERING PARAMETERS OF THE DETECTOR WITH AND WITHOUT NORMAL CELL.**

According to the figure (*Fig.8*) we clearly observed that the resonance frequency for reflection parameter  $S_{11}$  between normal cell (blue line) and without sample (red line) are analysed in the detector. The resonance frequencies are observed at 0.543 THz and 0.601THz in the detector with and without normal cells. By introducing the cells in our detector we found a remarkable sensitivity value of biological cells which is equal to 0.058 THz (58 GHz) that ensure our detector has a good sensitivity to the biological molecules and we have also observed the same observation for the transmission coefficient  $S_{21}$  and from the absorption graph shown in figure (*Fig .9*).

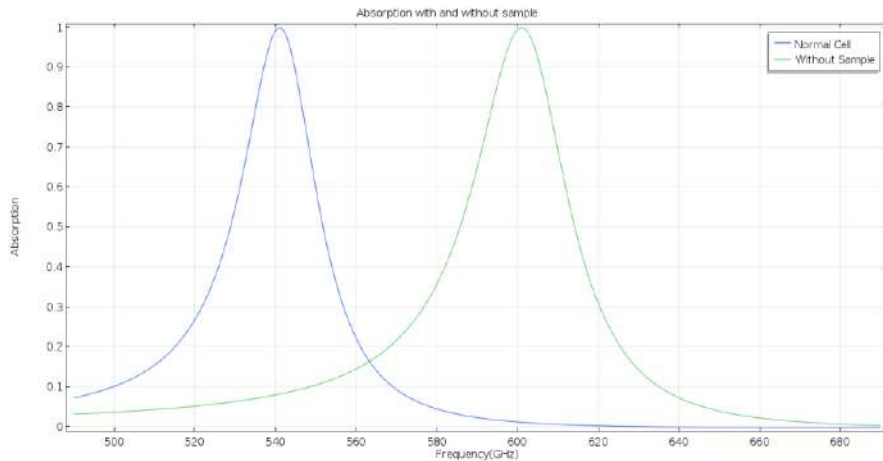


**FIG.9.ABSORPTION GRAPH FOR THE DETECTOR WITH AND WITHOUT NORMAL CELL.**

After simulating the various samples of cancer cells represented in the table (Table.1), we have obtained Reflection parameter  $S_{11}$  graph for various cells and Absorption graph for various cells as shown in figures(Fig .10, Fig .11).

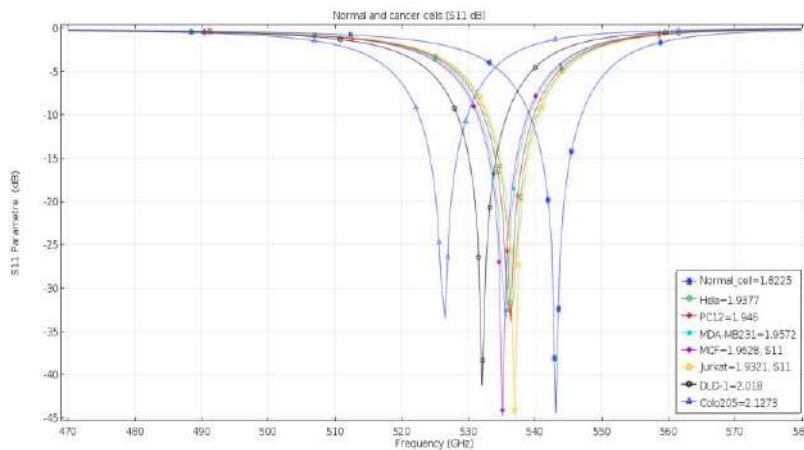


**FIG. 10. REFLECTION PARAMETER  $S_{11}$  FOR VARIOUS CELLS.**

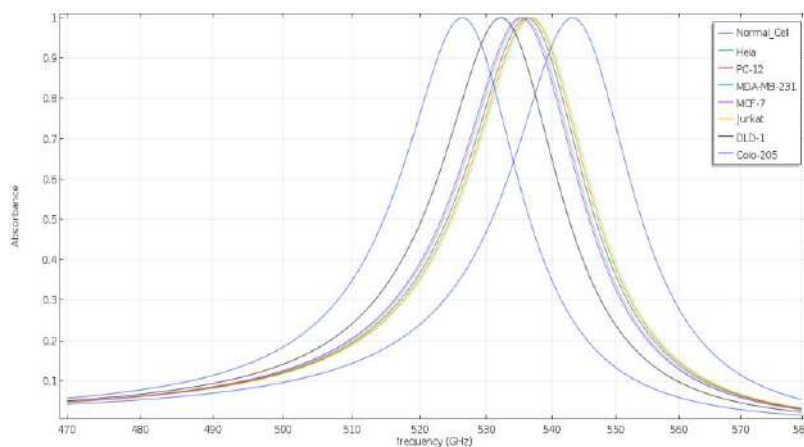


**FIG.11. ABSORPTION GRAPH FOR VARIOUS CELLS.**

According to the figure (Fig.10) we clearly see a remarkable high shifting in peaks of resonance frequencies between normal and various cancer cells and also low shifting between cells. From the variation of the resonance frequency it is possible to accurately distinguish healthy tissues from malignant ones. Also we observe a low shifting between Jurkat and Hela cells near to 0.5877 GHz (587.7MHz) and between PC12 and MDA-MB-231 equal to 0.615GHz (615MHz), and also between MCF-7 and MDA-MB-231 cells equal to 0.615GHz (615MHz), but this low shifting between various cells stay acceptable and it can increased while we use a high precision in a simulation with a high performance computer.

The curves shown in figure (Fig.11) illustrating the absorption for various cancer cells. According to this curves we observe that there is same shifting values between various cells as shown in the figure (Fig.10).

**4.1 Breast Cancer Cells Biosensor:**

In this part we specify our cancer cells detector as breast cancer biosensor only for two types of breast cancer cells MDA-MB-231 and MCF-7cells, then by varying the cells thickness from 2μm to 10μm with a step of 0.75μm in a sweep study in Comsol software we have obtained the resonance frequencies sweep as function of thickness sweep shown in the following figures.

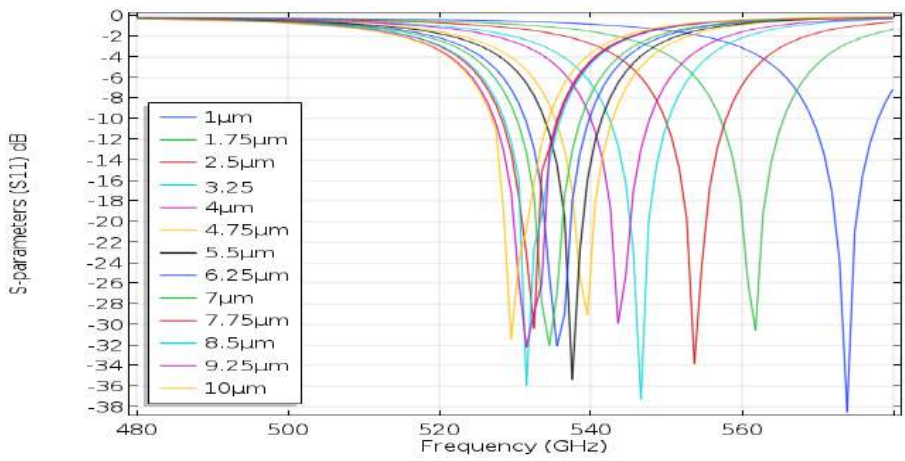


**FIG.12.VARIATION OF RESONANCE FREQUENCIES AS FUNCTION OF THICKNESS SWEEP FOR MDA-MB-231 CELL.**

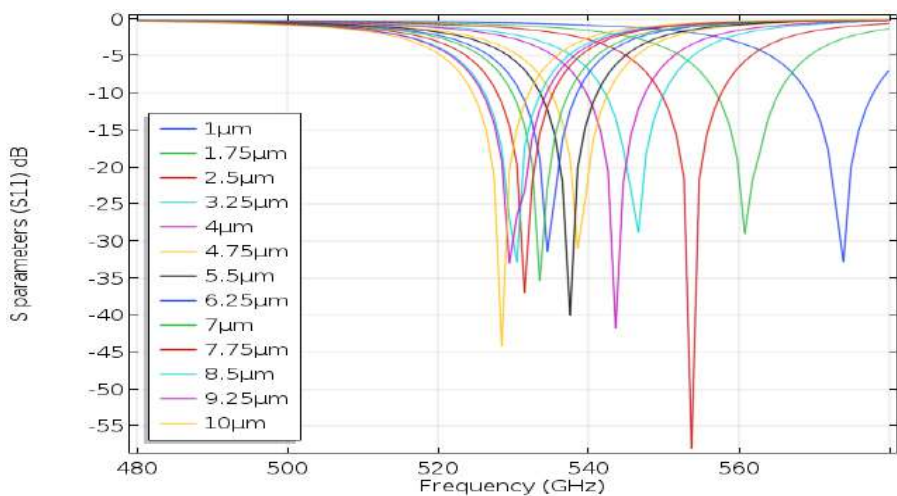


**FIG.13.VARIATION OF RESONANCE FREQUENCIES AS FUNCTION OF THICKNESS SWEEP FOR MCF-7 CELL.**

As shown in the figure (Fig.12) that represent the  $S_{11}$  parameter for MDA-MB-231 cell for various thickness, according to this figure we see a remarkable shifting to the low frequencies in a large range of frequency from 573.94 GHz to 529.49 GHz (44.45GHZ) that results help us to follow the development of cancer cell by following its thickness variation.

The figure (Fig.13) shows the  $S_{11}$  parameters for different thickness of breast cancer cell MCF-7, According to this figure we can see large range frequencies as shown on the curves of MDA-MB-231 cells (45.45GHz) and we can also see a remarkable difference between attenuations values. Simulated figures (Fig.12andFig.13) from our proposed Breast cancer biosensor, we have the obtained values of resonance frequencies peaks as function of thickness variations for MDA-MB-231 Cell and for MCF-7 cell.

**Table.II and Table.III values are tabulated from the simulated results of breast cancer biosensor**

Thickness( $\mu\text{m}$ )	Resonance frequency(GHz)
1	573.9393939
1.75	561.8181818
2.5	553.7373737
3.25	546.6666667
4	543.6363636
4.75	539.5959596
5.5	537.5757576
6.25	535.5555556
7	534.5454545
7.75	532.5252525
8.5	531.5151515
9.25	531.5151515
10	529.4949495

**TABLE.II. RESONANCE FREQUENCIES PEAKS AS A FUNCTION OF A THICKNESS SWEEP FOR MDA-MB-231 CELL.**

Thickness( $\mu\text{m}$ )	Resonance frequency(GHz)
1	573.9393939
1.75	560.8080808
2.5	553.7373737
3.25	546.6666667
4	543.6363636
4.75	538.5858586
5.5	537.5757576
6.25	534.5454545
7	533.5353535
7.75	531.5151515
8.5	530.5050505
9.25	529.4949495
10	528.4848485

**TABLE III. RESONANCE FREQUENCIES PEAK AS A FUNCTION OF A THICKNESS VARIATION FOR MCF-7 CELL.**

From the tables (Table.II and Table.III), we find that there is a difference between resonance frequencies peaks of two successive thicknesses near to 1 GHz, we accept it but with reservation this value can be increased while we use finer mesh, small step in thickness sweep and also by using computing station.

we have plotted the values of thickness sweep of various breast cancer cells as function of resonance frequencies from table II table III by curve fitting using Matlab Software that provide the best curves as shown in following figures (Fig.14, Fig.15).

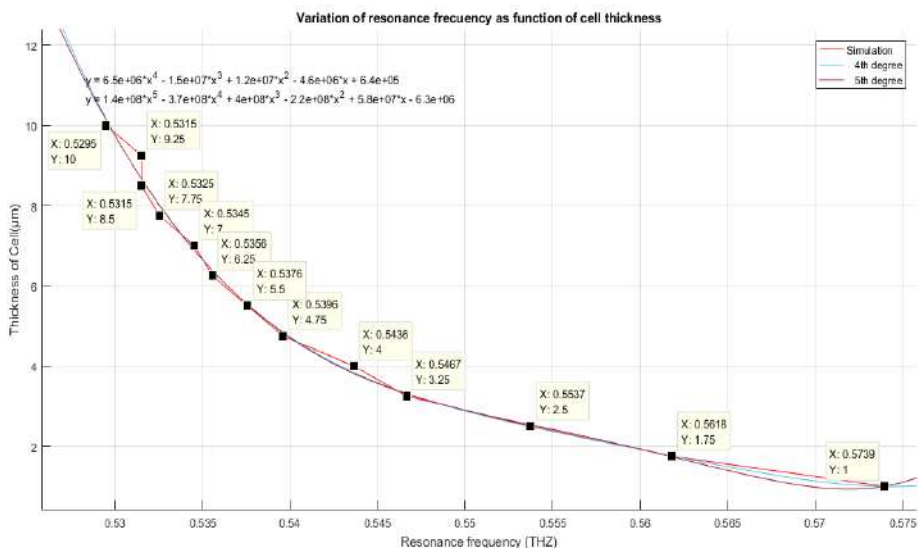


FIG.14.VARIATION OF THICKNESS VERSUS FREQUENCY FOR MDA-MB-231 CELL.

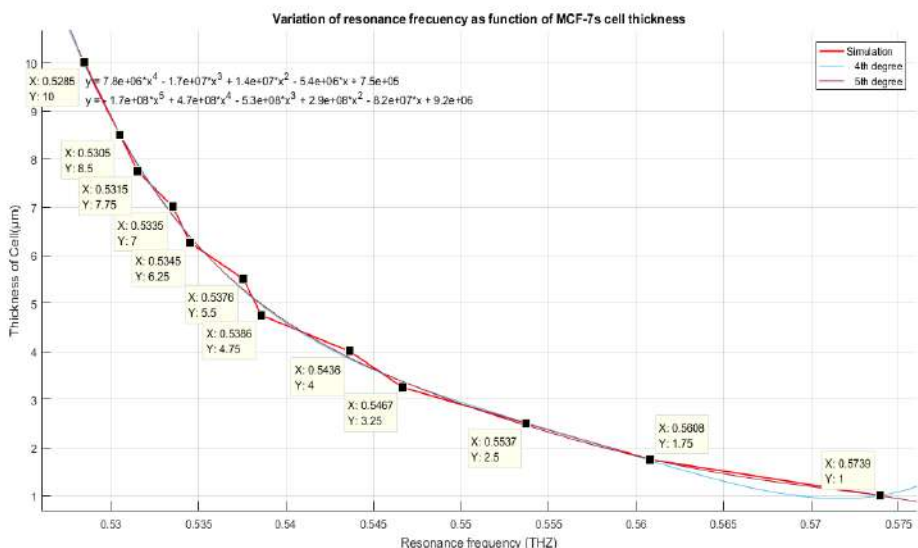


FIG.15.VARIATION OF THICKNESS VERSUS FREQUENCY FOR MCF-7 CELL.

By using mathematical interpolation [18], between results points with basic fitting methods on Matlab software we plotted the 4<sup>th</sup> and 5<sup>th</sup> order equations of the variation of thickness with respect to frequency peaks for both MDA-MB-231 and MCF-7 cells respectively [19, 20].

From the figures (Fig.14, Fig.15) we have observed the excellent curve between that points given by the fitting equations of 4<sup>th</sup> order (blue line Fig.14) for MDA-MB-231 cells and 5<sup>th</sup> order (violet line Fig.15) of MCF-7 cells.

The fitting equations of 4<sup>th</sup> and 5<sup>th</sup> order of MDA-MB-231 and MCF-7 cells are given by the following equations.

For MDA-MB-231

4<sup>th</sup> order:

$$T_{MDA}(f_r) = 6.5 * 10^6 (f_r)^4 - 1.5 * 10^7 (f_r)^3 + 1.2 * 10^7 (f_r)^2 - 4.6 * 10^6 (f_r) + 6.4 * 10^5 \quad (9.a)$$

5<sup>th</sup> order:

$$T_{MDA}(f_r) = 1.4 * 10^8 (f_r)^5 - 3.7 * 10^8 (f_r)^4 + 4 * 10^8 (f_r)^3 - 2.2 * 10^8 (f_r)^2 + 5.8 * 10^7 (f_r) - 6.3 * 10^6 \quad (9.b)$$

And for MCF-7 cells:

4<sup>th</sup> order:

$$T_{MCF}(f_r) = 7.8 * 10^6 (f_r)^4 - 1.7 * 10^7 (f_r)^3 + 1.4 * 10^7 (f_r)^2 - 5.4 * 10^6 (f_r) + 7.5 * 10^5 \quad (10.a)$$

5<sup>th</sup> order:

$$T_{MCF}(f_r) = -1.7 * 10^8 (f_r)^5 - 4.7 * 10^8 (f_r)^4 - 5.3 * 10^8 (f_r)^3 + 2.9 * 10^8 (f_r)^2 - 2.8 * 10^7 (f_r) + 9.2 * 10^6 \quad (10.b)$$

Depending on the equations (9.a, 9.b, 10.a, 10.b) we ensure that this biosensor can be used to track the evolution of the breast cancer cells thickness only by detecting their resonance frequencies peaks by the given equations.

## 5. RESULTS AND DISCUSSION

In this study we modelled and designed metamaterial based split ring resonator as biosensor with resonant frequencies in the terahertz regime (0.601 THz). All simulations within this study were performed by the use of the finite element method (FEM). Since SRRs are highly sensitive to the change in dielectric material the resonant frequencies shift proportional to the load of bio molecules. The obtained simulation results show that the resonant frequency shift strongly depends on the thickness. The desired resonance frequency value obtained from the simulation allows the proposed metamaterials based resonator structure increases the designing flexibility of biosensors, and dramatically improves their Performance with high sensitivity. The permittivity graph as function of frequency variation which it presents negative permittivity values that confirm the electric properties of metamaterials in the desired frequency range. The simulation results show that the resonance frequency of reflection parameter  $S_{11}$  from the curve equal to 0.601 THz with an attenuation of -29dB. We can see a remarkable high shifting in resonance frequencies between normal and various cancer cells and also low shifting between cancer cells from the Fig.10. We have obtained the resonance frequency variations as function of thickness sweep for MDA-MB-231 and MCF-7 cells from 1 $\mu$ m to 10 $\mu$ m by a step of 0.75 $\mu$ m. From this we can also analyse the growth of cancer cells by resonance frequency with thickness variations. We have obtained the double negative characteristics as the permittivity, permeability are negative, and the refractive index is negative in the THz region by Nicolson-Ross-Weir method (NRW) which ensure metamaterial characteristics in our proposed model.

It is found that our proposed design has its own advantages in terms we have obtained the perfect absorber in the terahertz region illustrating with shift in resonance frequency for various cancer cells. Our proposed structure of metamaterial based split ring resonator as biosensor possesses much higher sensitivity to detect the cancer cells for cancer diagnosis in the terahertz region.

## 6. CONCLUSION

The main focus of our study lies on the development of a theoretical biosensor device based on split ring resonator structures operating in the terahertz regime. We proposed metamaterial-based perfect absorbers with unit cell designs and simulated transmittances, reflectance and absorbance in order to assess the sensor functionality with higher sensitivity for detecting the cancer cells for cancer diagnosis in the terahertz region. Further the shifting of resonance frequency by varying thickness should be performed in order to confirm the cancer diagnosis, as well as electric properties of metamaterial behaviour in the desired frequency range confirm negative permittivity values. We have also successfully investigated the unique characteristics of the metamaterials, such as, negative permittivity, negative permeability and negative refractive index by using Nicolson Ross-Weir method (NRW) method.

These results have a potential application in cancer detection and diagnosis and can be useful in order to develop new diagnosis devices. In particular, split-ring resonators designed for operation in the terahertz regime open the road for the development of compact and cost efficient sensing devices. For real sensor applications like the detection of cancer cells for early diagnosis. Therefore the simulation outcomes indicate a high sensor functionality of our biosensor devices. The proposed structure has been successfully used as a resonator based metamaterial biosensor working in the THz regime. Biosensor applications in such areas as healthcare, environmental, industrial, security and defence, this is expected to achieve exponential growth over the upcoming years.

## ACKNOWLEDGMENTS

I would like to thank almighty god for his grace and also my guide Dr. K. S. Joseph Wilson, my Parents, N. Leebanon Poonkuil, Alfasid Badurudeen, Raj Kumar, my family members as well as all my friends for their consecutive support and guidance.

## REFERENCES

1. V.G. Veselago; The electrodynamics of substances with simultaneously negative value  $\epsilon$  and  $\mu$ , Sov. Phys. Uspekhy. 10 (4), 509-514, 1968.
2. Fang, N.; Lee, H.; Sun, C.; Zhang, X., Sub-diffraction-limited optical imaging with a silver superlens. Science 2005, 308, 534-537.
3. Chen, H. S.; Wu, B. I.; Zhang, B.; Kong, J. A., Electromagnetic wave interactions with a metamaterial cloak. Phys. Rev. Lett. 2007, 99, 063903.
4. Williams, C. R.; Andrews, S. R.; Maier, S. A.; Fernandez-Dominguez, A. I.; Martin Moreno, L.; Garcia-Vidal, F. J., Highly confined guiding of terahertz surface plasmon polaritons on structured metal surfaces. Nature Photonics 2008, 2, 175-179.
5. Alu, A.; Salandrino, A.; Engheta, N., Negative effective permeability and left handed materials at optical frequencies. Optics Express 2006, 14, 1557-1567.
6. Z. Jakšić, Z. Djurić, and C. Kment, "A consideration of the use of metamaterials for Sensing applications: Field fluctuations and ultimate performance," J. Opt. A: Pure Appl. Opt., vol. 9, pp. S377–S377, Sep. 2007.
7. S. He, Y. Jin, Z. C. Ruan, and J. G. Kuang, "On sub wavelength and open resonators involving metamaterials of negative refraction index," New J. Phys., vol. 7, no. 1, p. 210, Mar. 2005.
8. Gay-Balmaz, Philippe & Martin, Olivier. (2003). Electromagnetic resonances in individual and coupled split-ring resonators. Journal of Applied Physics - J APPL PHYS. 94. 10.1063/1.1497452.
9. M. Garcia and A. Jemal, "Global Cancer Facts and Figures 2011," Atlanta, GA: American Cancer Society, 2011.
10. Markus Wellenzohn, Martin Brandl, A theoretical design of a biosensor device based on Split ring resonators for operation in the microwave regime, Science Direct Procedia Engineering 120 (2015) 865 – 869.

11. C. Kenneth Diest, Numerical Methods for Metamaterial Design, Springer Dordrecht Heidelberg New York London, 2013, p.p.9-16.
12. Jayant G. Joshi, Shyam S. Pattnaik, Swapna Devi and Mohan R. Lohokare, Bandwidth Enhancement and Size Reduction of Microstrip Patch Antenna by Magnetoinductive Waveguide Loading, Wireless Engineering and Technology, 2(2), 2011, 37-44.
13. Bilkish Mondol, Zakir Hussain "Measurement of Cancer Cell Detection using Photonic Sensor" IJCAT International Journal of Computing and Technology, Volume 1, Issue 3, April 2014.
14. G.H. Markx, et al., The dielectric properties of biological cells at radiofrequencies: applications in biotechnology, Enzyme Microb. Technol. 25 (August (3-5)) (1999) 161-171.
15. Zhang, L.Y. & Morand du Puch, Christophe & Dalmay, Claire & Lacroix, Aurélie & Landoulsi, Alaeddine & Leroy, Jonathan & Mélin, Carole & Lalloué, Fabrice & Battu, Serge & Lautrette, Christophe & Giraud, Stéphanie & Bessaudou, Annie & Blondy, Pierre & Jauberteau, Marie & Pothier, Arnaud. (2014). Discrimination of Colorectal Cancer Cell Lines using Microwave Biosensors. Sensors and Actuators A: Physical. 216. 10.1016/j.sna.2014.03.022.
16. F. P. Bolin, L. E. Preuss, R. C. Taylor and R. J. Ference, "Refractive Index of Some Mammalian Tissues using a Fiber Optic Cladding Method," Applied Optics 28, 2297-2303 (1989)
17. Shiraga, Keiichiro & Ogawa, Yuichi & Suzuki, Tetsuhito & Kondo, Naoshi & Irisawa, Akiyoshi & Imamura, Motoki. (2014). Characterization of Dielectric Responses of Human Cancer Cells in the Terahertz Region. Journal of Infrared, Millimeter, and Terahertz Waves. 35. 10.1007/s10762-014-0067-y.
18. Barthelmann, Volker & Novak, Erich & Ritter, Klaus. (2000). High dimensional polynomial interpolation on sparse grids. Adv. Comput. Math. 12. 273-288. 10.1023/A: 1018977404843.
19. [https://www.mathworks.com/help/matlab/data\\_analysis/interactive-fitting.html](https://www.mathworks.com/help/matlab/data_analysis/interactive-fitting.html)
20. Mezache Z, Zara Ch, Larioui F, Benabdelaziz F, "Detection and analysis of human hemoglobin HB and HBO2 with new Nano-sensor based on chiral metamaterials", International Journal of Physical Research, 5(2), 36-38 (2017).